Self-Assembly Behavior of Poly(methacrylic acid-*block*-ethyl acrylate) Polymer in Aqueous Medium: Potentiometric Titration and Laser Light Scattering Studies

C. Wang,[†] P. Ravi,[†] K. C. Tam,*[,†] and L. H. Gan[‡]

Singapore-MIT Alliance, School of Mechanical and Production Engineering, and Natural Sciences, National Institute of Education, Nanyang Technological University, 50 Nanyang Avenue, Singapore 639798

Received: September 5, 2003; In Final Form: November 14, 2003

The self-assembling behavior of poly(methacrylic acid-*block*-ethyl acrylate) (P(MAA-*b*-EA)) copolymer synthesized via atom transfer radical polymerization (ATRP) was examined and compared with that of random and cross-linked MAA−EA copolymers. The polymer exists as spherical micelle containing 60 polymer chains. The micelle consists of a hydrophobic EA core surrounded by a hydrophilic MAA shell, which expands when the MAA segments are ionized. During the course of neutralization, the particle size increases from ∼22 nm at $\alpha = 0$ to 30 nm at $\alpha = 0.15$, thereafter it decreases to a minimum of ∼12 nm at $\alpha = 0.29$, suggesting that the polymer undergoes a structural change (expansion−dissociation) upon ionization. When α exceeds 0.6, the micelles completely disintegrate into single polymer chains.

Introduction

In recent years, much interest has been focused on the self-assembled structure of polyelectrolyte amphiphilic block copolymers in aqueous solution. The outstanding feature of these polymers is that they self-assemble to form micelles with well-defined size and shape. Furthermore, their characteristics may respond to external stimuli such as pH or addition of neutral salt, which makes them useful for specific applications.[1−3] Thus it is possible to tune the aggregate properties not only by varying the type of monomer, chain length, and proportion of the constituting blocks, but also by changing the pH or ionic strength of the solution.[2−4] Therefore amphiphilic block copolymers are able to provide broader applications than normal surfactants, such as nanoreactors, solubilization of drugs in controlled drug delivery, and DNA carriers.[5−8]

The self-assembling of polyelectrolyte block copolymers is mainly controlled by hydrophobic interaction and electrostatic repulsion. In aqueous solution, the nonionic (usually hydrophobic) moieties form the core of the micelle surrounded by a corona composed of the ionic blocks.[9] In addition, due to the poor compatibility between ionic and nonionic blocks, the micellization occurs at very low polymer concentration with a critical micelle concentration (CMC) as low as $\sim 10^{-8}$ M.[10,11] Stepanek et al.[12] observed that the pH and ionic strength strongly altered the CMC values and physical properties of the micelle. For example, the hydrodynamic radius of micelles of poly(styrene-*b*-methacrylic acid) (P(sty-*b*-MAA)) increases from ∼50 to ∼80 nm as pH increases from 4 to 8, resulting from the enhanced electrostatic repulsion upon neutralization of MAA blocks.[10] Systematic studies on the block polyelectrolyte of poly(styrene-*b*-acrylic acid) (P(sty-*b*-AA)) and P(sty-*b*-MAA) with respect to micellar size and structure have been reported.[13,14] As proposed by Eisenberg and co-workers, the polymers form star or crew-cut micelles depending on the hydrophobic−hydrophilic balance between the two blocks.[15] Müller and co-workers reported that poly(isobutylene-*b*-methacrylic acid) (P(IB-*b*-MAA)), diblock copolymer forms core−shell structure with a dense core of PIB blocks and a swollen corona of PMAA blocks.[11] The block copolymers of poly(ethylene glycol) (PEG) based poly(methacrylic acid) (PMAA) derivatives were also found to form pH-dependent core−shell structure, which may offer promising characteristics for the delivery of charged compounds (e.g., DNA).[16]

The micellar conformation of block polyelectrolytes is controlled by a number of contributing factors, which force the polymers to form more complicated micellar structures besides the simple core−shell structure. A cylindrical core−shell structure was reported by Müller and co-workers for P(sty-*b*-AA) block copolymers.[17] Schuch et al. proposed the formation of a small vesicle-like structure for P(IB-*b*-MAA) in aqueous medium.[11] ABC triblock copolyampholytes of the type poly[5-(*N*,*N*-dimethylamino)isoprene-*block*-styrene-*block*-methacrylic acid] (AiSA) were found to form a large vesicular structure with almost pH-independent radius in aqueous solutions.[18] The formation of three-layer vesicular micelle from pH responsive tri-block copolymer of poly(styrene-*b*-2-vinylpyridine-*b*-ethylene oxide) in water was reported by Gohy et al.[19] It was also demonstrated that the pH sensitive poly(2-vinylpyridine) shell is useful to tune the size of the vesicle, which is mainly attributed to the electrostatic repulsion between the charged polyelectrolyte chains.[19] Onion-like multilayer micelles were observed in the aqueous solution of block polyelectrolytes based on poly(styrene-*b*-2-vinylpyridine) and poly(2-vinylpyridine-*b*-ethylene oxide) by Talingting et al.[20]

Besides the micellar structure, the kinetics of macromolecular exchange between micelle and solution for block polyelectrolyte is another point of interest for many researchers. Tuzar and co-workers reported fluorescence studies on the amphiphilic poly(methacrylic acid-*b*-styrene-*b*-methacrylic acid) (P(MAA-*b*-sty-

* Corresponding author. E-mail: mkctam@ntu.edu.sg.
[†] Singapore-MIT Alliance, School of Mechanical and Production Engineering.
[‡] Natural Sciences, National Institute of Education.

10.1021/jp036648q CCC: $27.50
Published on Web 01/07/2004

b-MAA)) micelles, where they observed a significant fraction (ca. 20−30%) of pyrene molecules on or near the polystyrene−water interface, and the diffusion of the probe out of the micelle is the rate-determining step in the release and exchange of large hydrophobes.[21,22] Tuzar et al. also studied the behaviors of di- and triblock copolymers of PMAA and PS in dioxane/water mixtures. When the polymers were dissolved in dioxane-rich mixture, a dynamic equilibrium between micelles and unimers was observed. But as the polymers were transferred to water-rich mixtures via dialysis, frozen micelles behaving like autonomous particles were detected.[23]

The dynamic equilibrium between micelles and unimers not only depends on the hydrophobic−hydrophilic balance but also strongly depends on the T_g of the hydrophobic block. Most of the reported studies focused on diblock polyelectrolytes, which contain hydrophobic segments with high T_g, where the hydrophobic core is frozen because the lifetime of hydrophobic segments in the micellar core is extremely long. Studies on the micellization behavior of polyelectrolytes with lower T_g should be interesting as such systems find potential applications in drug delivery where hydrophobic cores with lower T_g's are preferred as they are more permeable than the glassy ones.[24] In this study, we have chosen a hydrophobic core with a lower T_g, such as poly(ethyl acrylate) (PEA) ($T_g \sim -31$ °C) where the block copolymer of P(MAA-*b*-EA) could form a more dynamic and permeable hydrophobic core compared to P(MAA-*b*-MMA) or P(MAA-*b*-sty). We reported, for the first time, the micellization behavior of poly(methacrylic acid-*block*-ethyl acrylate), P(MAA-*b*-EA), in aqueous solution and compared its aggregation behavior to that of random and cross-linked MAA/EA copolymer.

Experimental Section

Materials. *tert*-Butyl methacrylate (tBMA, Aldrich, 98%) was passed through a basic alumina column, stirred over CaH_2 and distilled under reduced pressure. Ethyl acrylate (EA, Aldrich, 99%) was stirred over CaH_2 and distilled under vacuum. CuBr (99.99%), CuCl (99.98%), *N*,*N*,*N*′,*N*″,*N*″-pentamethyldiethylenetriamine (PMDETA), *N*,*N*,*N*′,*N*′,*N*″,*N*″-hexamethyltriethylenetetramine (HMTETA), *ρ*-toluenesulfonyl chloride (*ρ*-TSCl), and anisole were purchased.

The random and cross-linked MAA−EA copolymers were synthesized by Dow Chemicals using the emulsion polymerization technique; the detailed polymerization procedure and characterization of these polymers are published elsewhere.[25,26] Atom transfer radical polymerization with the group protecting technique was used to synthesize P(MAA-*b*-EA). To synthesize the block copolymer, poly(*tert*-butyl methacrylate) (PtBMA) macroinitiator was first prepared as reported in our previous paper.[27] A known amount of Cl-terminated P(tBMA) as a macroinitiator and CuBr were charged into a Schlenk flask and dissolved in a minimum amount of degassed benzene. Monomer was introduced using an Ar-washed syringe. The reaction mixture was degassed three times using freeze−pump−thaw cycles. Finally, degassed ligand (PMDETA) was introduced using an Ar-purged syringe and the flask was placed in an oil bath, which was thermostated at 60 °C. After the reaction was complete, the catalyst was removed by passing through an alumina column and the polymer was recovered by precipitation in excess cold methanol, filtered, and dried under vacuum. Subsequently, the *tert*-butyl groups of the P(tBMA) blocks were hydrolyzed in the presence of concentrated hydrochloric acid in dioxane at 85 °C for 5 h to form PMAA blocks. FT-IR (KBr-pellet) showed the broad peak at 3500 cm^{-1}, which is the characteristic absorption for carboxylic acid, and the content of the acid was quantified by potentiometric titration.

Polymer Characterization. *Gel Permeation Chromatography.* The polymer molecular weights and molecular weight distributions were determined using gel permeation chromatography (GPC). An Agilent 1100 series GPC system equipped with a LC pump, PLgel 5 μm MIXED-C column, and RI detector was used. The column was calibrated with narrow molecular weight polystyrene standards. HPLC grade THF stabilized with BHT was used as a mobile phase. The flow rate was maintained at 1.0 mL min^{-1}.

Nuclear Magnetic Resonance Spectroscopy (NMR). The ^1H NMR spectrum for the precursor P(tBMA-*b*-EA) block copolymer was measured using a Brüker DRX400 instrument in $CDCl_3$. The ^1H NMR spectrum of the block copolymer allows the molar composition to be determined from the relative intensity at 1.42 ppm ($-C(CH_3)_3$ of the tBMA block) and 4.02 ppm ($-OCH_2$ of EA block).

Potentiometric Titration. An ABU93 Triburet Titration System equipped with Radiometer pHG201 pH glass and Radiometer REF201 reference electrodes was used to conduct the potentiometric titrations. All the titrations were performed under constant stirring at 25 °C, in a titration vessel filled with 100 mL of 0.1 wt % polymer solution. A 1 M standard NaOH solution (from Merck) was used, and 1 min of lag time was allowed between two dosages to ensure that the reaction has reached equilibrium.

Laser Light Scattering. The laser light scattering experiments were conducted using the Brookhaven laser light scattering system. This system consists of a BI200SM goniometer, BI-9000AT digital correlator and other supporting data acquisition and analysis software and accessories. An argon-ion vertically polarized 488 nm laser was used as the light source. In DLS, the time correlation function of the scattered intensity $G_2(t)$, which is defined as $G_2(t) = I(t)\ I(t + \Delta t)$ where $I(t)$ is the intensity at time t and Δt is the lag time, is analyzed using the inverse Laplace transformation technique (REPES in our case) to produce the distribution function of decay times. The concentration of the polymer solutions investigated by light scattering is 0.04 wt %, which is in the dilute solution regime where the behavior of individual particles can be characterized. Several measurements were performed at varying scattering angles for a given sample to obtain an average hydrodynamic radius. The variation in R_h values was found to be small.

Results and Discussion

Polymer Synthesis. Though homopolymerization of tBMA by the ATRP technique has been reported previously,[25,28] block copolymerization with EA has not been studied so far. Chlorine-terminated PtBMA macroinitiator end group was synthesized using *ρ*-toluenesulfonyl chloride (TsCl) as the initiator and CuCl complexed by HMTETA as the catalyst in 50% vol anisole at 90 °C. It has been demonstrated that TsCl acts as a better initiator than a propagator for reactions involving methacrylates and styrenes. Using TsCl, well-defined homopolymer was synthesized with $M_n = 6000$ Da and a polydispersity index (PDI) of 1.12. The resulting P(tBMA)−Cl was used as a macroinitiator to prepare block copolymer with EA. Block copolymerization was carried out using CuBr as a cross catalyst complexed with PMDETA in benzene. The molecular mass of the P(tBMA-*b*-EA) was $M_n = 8000$ Da with PDI of 1.3. The block lengths of the copolymer calculated from ^1H NMR spectrum were 43 and 19 for tBMA and EA, respectively.

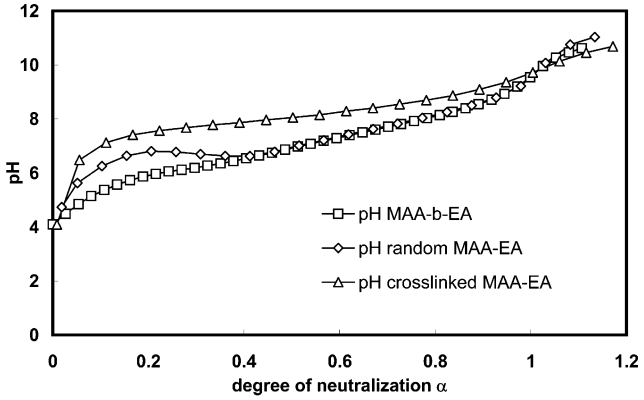

Figure 1. Comparison of pH curves for 0.1 wt % aqueous solutions of block, random, and cross-linked MAA−EA copolymers.

Potentiometric Titration of Random, Cross-Linked, and MAA-*b*-EA Copolymers. The degree of neutralization, α, of carboxylic groups is defined by

$$\alpha = \frac{[\mathrm{BASE}] + [\mathrm{H^+}] - [\mathrm{OH^-}]}{C_{\mathrm{COOH}}} \tag{1}$$

where [BASE], [H^+], and [OH^-] are the molarities of added base, free hydrogen ion, and hydroxide ion, respectively, and C_{COOH} is the total concentration of methacrylic acid groups expressed in moles per liter. With this definition, the polyacid is completely neutralized at $\alpha = 1$. Figure 1 shows the pH curves plotted against α obtained from titrating 1 M NaOH into the aqueous solutions of block, random and cross-linked MAA−EA copolymer. The three copolymers possess identical MAA:EA molar ratio of approximately 7:3 and the concentration of the solutions is 0.1 wt %. As shown in the figure, each of the MAA−EA copolymers has its unique titration profile. For the random MAA−EA copolymer (open diamond), pH exhibits a plateau in the range of α from ∼0.1 to 0.4; thereafter it increases progressively until the neutralization process is completed at a well-defined equivalence point of $\alpha = 1$. The plateau region in the pH curve suggests a two-step dissociation and a conformational transition of the polymer upon neutralization, which has been extensively studied by our research group.[25,26] For cross-linked MAA−EA copolymer, the pH increases progressively with α, indicating that the polymer dissociates in one step and may exhibit a gradual expansion instead of a drastic conformational change upon neutralization.[29−31] For P(MAA-*b*-EA) block copolymer, the pH increases gradually with α over the entire course of neutralization. It is noted that the pH curve exhibits a gentle slope in the α range from ∼0.1 to 0.4, and the slope becomes steeper with increasing α until the complete neutralization is reached. These features suggest that the aggregate of the block copolymer may undergo a structural change in the α range 0.1−0.4.

The potentiometric titration of polyelectrolyte solution is usually treated in terms of the negative logarithm of the apparent dissociation constant (pK_a), which is more informative than the pH curves. The pK_a is described by the Henderson−Hasselbalch equation:

$$\mathrm{p}K_a = \mathrm{pH} + \log\frac{1-\alpha}{\alpha} \tag{2}$$

The negative logarithm of the intrinsic dissociation constant, namely pK_0, can be determined by extrapolating the pK_a curve to $\alpha = 0$. It is known that the intrinsic dissociation constant K_0 is related to the standard change of the free energy (ΔG_0) for the dissociation of H^+ from an isolated acid group, whereas the apparent dissociation constant K_a contains an additional contribution, ΔG_{el}, which is related to the extra work to overcome the electrostatic attraction between the H^+ and $\sim COO^-$ when transferring the proton from the polyanion to the bulk.[29−32] Thus pK_a can be written as a sum of two terms:

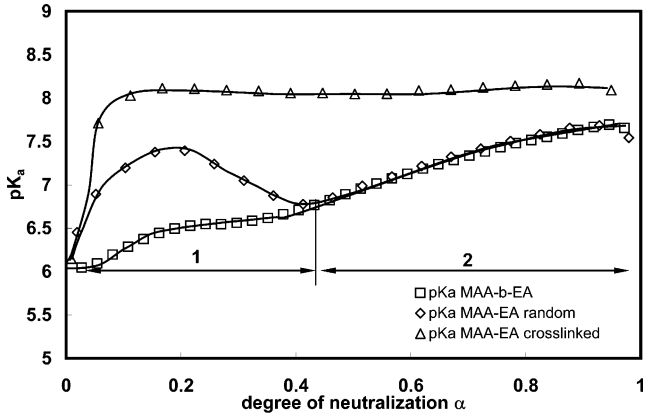

Figure 2. Comparison of pK_a curves of the block, random, and cross-linked MAA−EA copolymers.

$$\mathrm{p}K_a = \mathrm{p}K_0 + 0.4343\frac{\mathrm{d}G_{el}}{RT\,\mathrm{d}\alpha} \tag{3}$$

where R is the gas constant and T is the absolute temperature. ΔG_{el} (from $\alpha = 0$ to 1) can be calculated from the graphical integration of the extended Henderson−Haselbalch equation:[33−36]

$$\Delta G_{el} = 2.30RT\int_0^1 [\mathrm{p}K_{(\alpha)} - \mathrm{p}K_0]\,\mathrm{d}\alpha \tag{4}$$

Figure 2 shows the comparison of the pK_a curves of P(MAA-*b*-EA) block copolymer, random MAA−EA copolymer and cross-linked MAA−EA copolymer. The pK_a curve of the random MAA−EA copolymer (open diamond) exhibit a negative slope between two inflection points in the range of α from 0.2 to 0.4, which corresponds to the plateau region shown on the pH curve plotted in Figure 1. This feature is attributed to the discontinuous conformational transition of polymer particles in the course of neutralization, which has been reported in our previous studies.[25,26,37] The polymer expands initially from insoluble latex particle to swollen hydrated random particles driven by electrostatic repulsion between negatively charged carboxylate groups. Thereafter the swollen particles disintegrate into several smaller clusters when the electrostatic repulsion exceeds the hydrophobic attraction between EA groups. Moreover, the conformational change that unfolds and expands the compact latex particle is favorable for the dissociation of protons from the polyanions, which is reflected by the negative slope observed in the pK_a curve.[25,26] Compared with the pK_a curve of random MAA−EA copolymer, the pK_a curve of the cross-linked MAA−EA copolymer (open triangle) is flat over a wide range of α (from 0.1 to 1). When the polymer chains are chemically bonded by cross-linkers, charging of the polymer chains may only expand the particle to a certain extent, whereas the general structure of the latex particle is retained. Therefore no conformational change that alters the dissociation of the polyacid is involved during neutralization, thus the deprotonation of carboxylic groups occurs in one step and is essentially independent of α.

For the block P(MAA-*b*-EA) copolymer, the pK_a (open square) increases in the α range from 0 to ∼0.16, it levels off from α ∼ 0.16 to 0.4; thereafter it merges with the pK_a curve of the random copolymer and increases nearly linearly until the full neutralization (α = 1) is reached. The pK_a curves of the block and random copolymer can be categorized into two stages by the inflection point at α = 0.4, as depicted in Figure 2. The pK_a value of the block copolymer is considerably lower than that of the random copolymer in stage 1, indicating that the dissociation of carboxylic groups is more favorable for the block copolymer. This implies that the block copolymer may exist as a core−shell micelle, where the hydrophobic EA segments aggregate to form a hydrophobic core with a corona consisting of MAA segments. Thus, it is easier for the carboxylic groups in the corona of the block copolymer micelles to be deprotonated compared to random copolymer, where some of the carboxylic groups are trapped inside the compact latex particles and are not readily accessible. Moreover, the pK_a curve of the block copolymer also exhibits a slope change at α ∼ 0.2; however, it is less steep compared to the random copolymer. This may indicate a structural change driven by electrostatic repulsion between the charged carboxylate groups. However, it is not possible to elucidate the structural change exhaustively on the basis of the potentiometric titration study alone; hence light scattering was used to obtain additional information on the microstructure. A detailed discussion on the polymer conformation will be given later. In stage 2, the pK_a curves of block and random MAA−EA copolymers merge, signifying that the dissociation processes of these two polymers are identical and are independent of the structure of polymer aggregates. The continuous increase of pK_a in stage 2 suggests that it is more difficult to extract proton from the carboxylic groups. The addition of NaOH neutralizes and ionizes the carboxylic groups and consequently increases the electrostatic potential on the surface of the polymer aggregates. Thus, the proton−polyanion electrostatic attraction is enhanced, which is unfavorable for the dissociation of these carboxylic groups.

The pK_0 values for the three polymers can be determined by extrapolating the pK_a curves to α = 0. It is found that the three polymers have identical pK_0 value of approximately 6.02, suggesting that the spontaneous dissociation of carboxylic groups and the standard free energy change (ΔG_0) are only dependent on the environment of the protons. By performing graphical integration using eq 4, the ΔG_{el} were determined to be 9.43, 3.95, and 2.39 kJ for the cross-linked, random, and block MAA−EA copolymers, respectively. The difference in the ΔG_{el} between the block, random, and cross-linked copolymers is attributed to the different microstructures of the polymer aggregates in aqueous solutions. The cross-linked copolymer possesses the highest ΔG_{el}, because it remains as insoluble latex particle even at full neutralization, and this hinders the carboxylic groups from reacting with NaOH and larger amounts of work is required for dissociation. The random copolymer expands from insoluble latex particle to swollen random coil upon neutralization, thus a lower ΔG_{el} is required because of its relatively open structure compared to the cross-linked system.[25,26,32] For block copolymer, the carboxylic groups are distributed on the shell layer of the aggregate and are accessible to the base; thus it is more favorable for dissociation and less work is required to extract the proton from the polyanion.

Dynamic Light Scattering. Dynamic and static light scattering were used to measure the particle size of the P(MAA-*b*-EA) polymer at different α values. The relaxation time distribution functions obtained from DLS measurements at scattering angle of 90° for the polymer solutions at different α values are shown in Figure 3. The distribution function is unimodal and shifts to higher relaxation time as α increases from 0 to ∼0.15, corresponding to the expansion of polymer particles driven by the electrostatic repulsion between ionized carboxylate groups. With further addition of NaOH, the relaxation time decreases and the scattering intensity drops from 360 to 83 kcps until α reaches ∼0.3, which may be attributed to the disintegration of expanded polymer particle into smaller aggregates. When α exceeds ∼0.6, the scattering intensity drops to less than 30 kcps, and well-defined $g_2(t)$ correlation function cannot be obtained. This suggests that the electrostatic repulsion between the MAA blocks may have exceeded the hydrophobic attraction between EA blocks and the micelles dissociate into single polymer chains, resulting in a large drop in the scattering intensity. Figure 4 shows the distribution functions of the polymer solution of α = 0.22 measured at different scattering angles. Each of the distribution functions is unimodal and shifts to higher relaxation time with decreasing scattering angles. Figure 5 shows the dependence of decay rate Γ on q^2, where q is the scattering vector defined as $q = (4\pi n \sin(\theta/2)/\lambda)$ (where n is the refractive index of the solution, θ is the scattering angle, and λ is the wavelength of the incident laser light in a vacuum). Decay rate Γ exhibits good linear relationship with q^2, which confirms that the distribution function is caused by the translational diffusion of polymeric micelles.

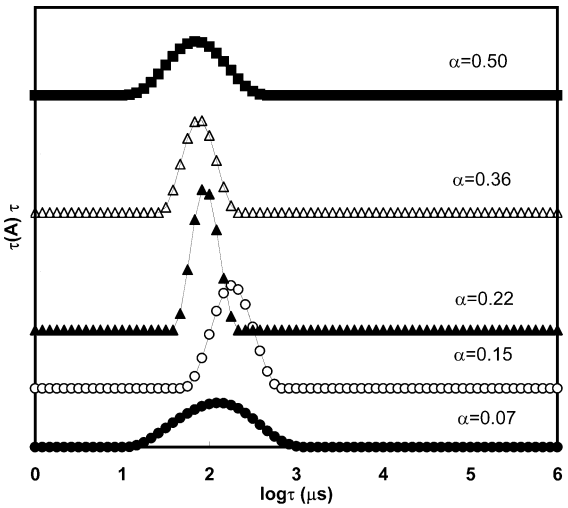

Figure 3. Characteristic relaxation time distribution functions obtained from DLS for 0.02 wt % P(MAA-*b*-EA) polymer solution at different α values.

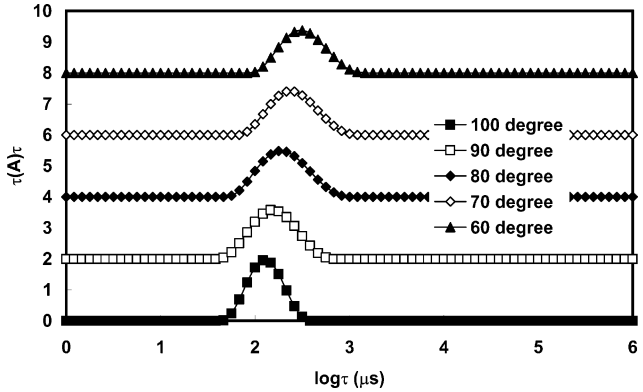

Figure 4. Relaxation time distribution functions for 0.02 wt % P(MAA-*b*-EA) polymer solution at α = 0.22 measured at different scattering angles.

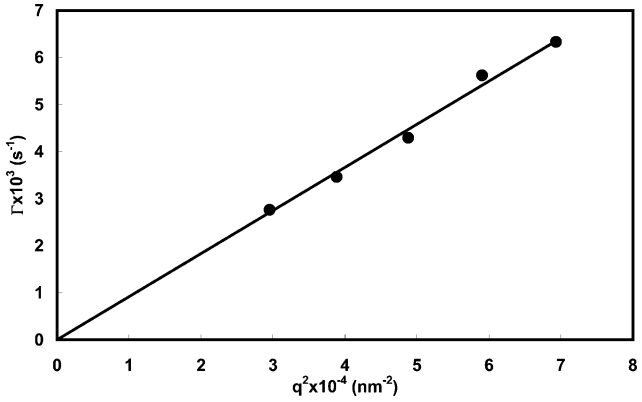

Figure 5. Dependence of decay rate Γ on q^2 for 0.02 wt % P(MAA-*b*-EA) polymer solution.

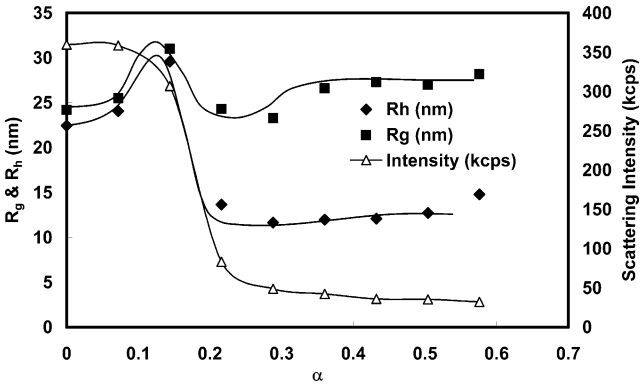

Figure 6. Dependence of R_h^{app}, R_g, and scattering intensity on α for 0.02 wt % P(MAA-*b*-EA) polymer solution.

The apparent hydrodynamic radius was determined from the Stokes−Einstein equation:

$$R_h = \frac{kTq^2}{6\pi\eta\Gamma} \tag{5}$$

where k is the Boltzmann constant, q is the scattering vector, η is the solvent viscosity, and Γ is the decay rate. The hydrodynamic radius (R_h^{app}) together with the scattering intensity was plotted against α in Figure 6. At α = 0, the particle size and scattering intensity is 22.5 nm and 360 kcps, respectively, which represents the compact polymer particle. When NaOH was titrated into the polymer solution, MAA segments are progressively neutralized and the polymer particle swells, driven by the electrostatic repulsion between the ionized carboxylate groups, resulting in the increase of R_h^{app} from 22.5 to 30.0 nm as α increases from 0 to 0.15. Thereafter the R_h^{app} decreases rapidly with α and reaches its minimum of 11.7 nm at α ∼ 0.3, which is accompanied by a decrease in the scattering intensity from 307 to 49 kcps, characterizing the disintegration of swollen polymer particles into smaller micelles caused by the overwhelming electrostatic repulsion between the charged MAA blocks. Comparison of Figure 6 and Figure 2 confirmed that the slope change and the plateau on the pK_a curve from α ∼ 0.1 to ∼0.3 corresponds to the structural change (swelling−disintegration) of polymer particles that occurs in the early stage of neutralization. With further addition of NaOH, R_h^{app} remains essentially constant at ∼12 nm, and the scattering intensity decreases slightly to 32 kcps. When α reaches ∼0.6, the scattering intensity becomes extremely low and the $g_2(t)$ correlation function cannot be determined, indicating the dissociation of micelles into single polymer chains. It is known that the association behavior of the P(MAA-*b*-EA) block copolymer is controlled by the competition between the electrostatic repulsion of charged MAA segments and hydrophobic attraction of EA segments. For the P(MAA-*b*-EA) block copolymer in our case, both the molecular weight and the EA molar percentage is relatively low (30% approximately); therefore the hydrophobicity of the EA blocks may not be sufficient to maintain the micellar structure when the polymer chains are highly charged, and the polymer micelle dissociates into single chains at high α. It is interesting to compare the association behavior of P(MAA-*b*-EA) with that of P(MAA-*b*-MMA).[37] The P(MAA_{102}-*b*-MMA_{10}) block copolymer retains its core−shell structure even when the polymer chains are highly charged (α = 1). The high stability of the P(MAA_{102}-*b*-MMA_{10}) is attributed to the PMMA block, whose T_g of 120 °C produces a glassy core, which minimizes chain mobility and results in "frozen micelles". However, the T_g of PEA block is low (−31 °C) and the polymer chain exchange rate between micelles and unimers is extremely fast. This dynamic equilibrium is controlled by the competition between electrostatic repulsion of MAA blocks and hydrophobic attraction of EA blocks, and the micelles may completely dissociate into single polymer chains when the electrostatic repulsion is sufficiently strong at high α.

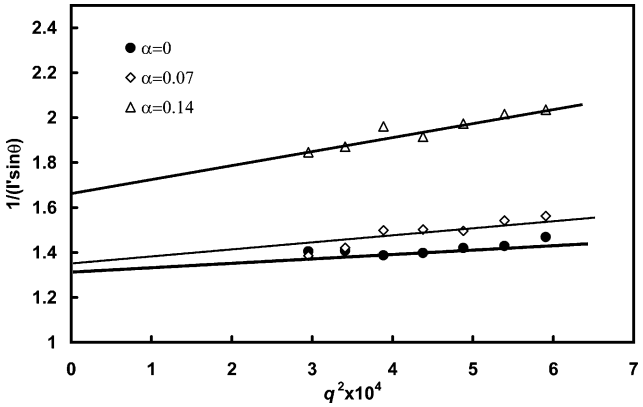

Figure 7. Dependence of $1/(I' \sin\theta)$ on q^2 for 0.02 wt % P(MAA-*b*-EA) solution at α = 0, α = 0.07, and α = 0.14.

Static Light Scattering. Static light scattering (SLS) measurements were performed on the P(MAA-*b*-EA) block copolymer to obtain the *z*-average radius of gyration (R_g^{app}) at various α values. It should be noted that R_g cannot be measured at α higher than 0.15 because the particle size is smaller than one-twentieth of the incident wavelength in diameter (24.4 nm). At higher α, the scattering intensities become very weak and the angular dependence of Rayleigh ratio is not reliable for determining R_g. Figure 7 shows the plots of $1/(I' \sin\theta)$ versus q^2 for P(MAA-*b*-EA) at α = 0, α = 0.07, and α = 0.14 together with the linear fitting of the plots, where the slopes of the fitted line give the apparent value of R_g and the intercept represents the apparent molar mass of the micelle. The dependence of R_g on α is also shown in Figure 6, where both R_h and R_g exhibit identical trends in the early stage of neutralization, R_g increasing from ∼24.2 to ∼31.0 nm as α increases from 0 to ∼ 0.15, which represents the expansion of polymer particles upon ionization.

The weight-average molar mass (M_w) of the micelles can be obtained from SLS measurements based on the Debye equation:

$$\frac{KC}{R(q)} = \frac{1}{M_w}\left(1 + \frac{1}{3}R_g^2 q^2\right) + 2A_2C \tag{6}$$

where K is an optical parameter ($K = 4\pi^2 n_{tol}^2 (dn/dc)^2 / N_A\lambda^4$, where n_{tol} is the refractive index of toluene (1.494), dn/dc is the refractive index increment of the polymer measured using

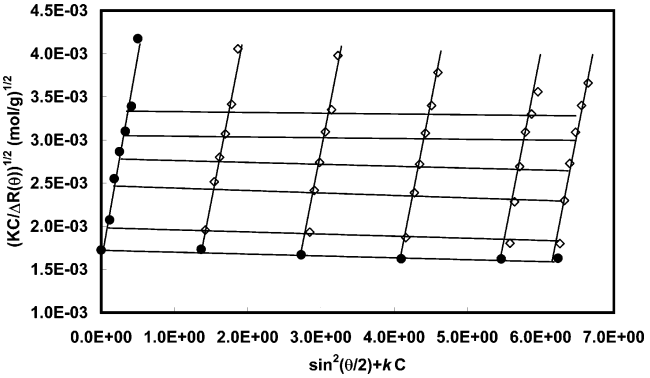

Figure 8. Berry plot ($KC/\Delta R(\theta)$ vs ($\sin^2(\theta/2) + kC$)) of P(MAA-*b*-EA) at $\alpha = 0.15$.

BI-DNDC, N_A is Avogadro's constant, and λ is the wavelength), C is the concentration of the polymer solition, $R(q)$ is the Rayleigh ratio, q is the scattering vector, and A_2 is the second virial coefficient. The absolute excess time-averaged scattered intensity, i.e., the Rayleigh ratio $R(q)$, is expressed by

$$R(q) = R_{\text{tol},90}\left(\frac{n}{n_{\text{tol}}}\right)^2 \frac{I - I_0}{I_{\text{tol}}} \sin\theta \qquad (7)$$

where $R_{\text{tol},90}$ is the Rayleigh ratio of toluene at measurement angle 90° with a value of 40×10^{-6} cm^{-1}, n is the refractive index of the solvent, I, I_0 and I_{tol} are the scattered intensities of the solution, solvent, and toluene respectively, and θ is the measurement angle. The Berry plot was constructed by plotting $[KC/R(q)]^{1/2}$ measured at different concentrations and angles against $\sin^2(\theta/2) + kC$, where k is an arbitrary constant. Extrapolating $[KC/R(q)]^{1/2}$ to zero concentration or zero angle yields M_w, R_g, and A_2. Figure 8 shows the Berry plot of P(MAA-*b*-EA) block copolymer at $\alpha = 0.14$, obtained from the SLS measurements at scattering angles ranging from 30 to 100° at 10° intervals, and the polymer concentration was varied from 0.2 to 0.9 mg/mL (0.2, 0.4, 0.6, 0.8, and 0.9 mg/mL). The second virial coefficient A_2 obtained from the Berry plot is $-3.55 \times 10^{-4} \pm 2.40 \times 10^{-4}$ (cm^3 mol)/g^2, indicating that water is a poor solvent for the polymer at $\alpha = 0.14$, where most of the carboxylic groups still remain uncharged and the polymer chains are fairly hydrophobic. The molar mass (M_w) of the micelle determined from the Berry plot is 3.36×10^5 g/mol ± 9.6%, and the aggregation number N_{agg} was determined to be 60 ± 6, where the molecular mass of a single polymer chain is 5600 Da according to GPC measurement. This aggregation number and the hydrodynamic radius revealed by DLS agree with the values for the spherical micelle that forms the core−shell structure, which contains 15−60 molecules per micelle with a hydrodynamic radius of 10−30 nm.[38] Combination of Figures 7 and 8 provides the variation of molar mass and aggregation number of the P(MAA-*b*-EA) micelle in the early stage of neutralization (from $\alpha = 0$ to 0.15). Initially, the micelle contains approximately 75 polymer chains and the N_{agg} remains constant from $\alpha = 0$ to $\alpha = 0.07$; with further addition of NaOH, which continuously ionizes the polymer, several polymer chains escape from the micelles and the N_{agg} decreases to 60 when α reaches 0.14. N_{agg} was not detectable beyond $\alpha = 0.15$; however, it is reasonable to assume that more polymer chains are released from the micelles into the solution due to electrostatic repulsion and solubilization of MAA blocks, causing complete demicellization of the polymer at $\alpha = 0.6$ as revealed by DLS. It should be stressed that the association behavior of block copolymers is complicated and is largely dependent on the block architecture, molecular weight, and method of solution preparation, and the aggregation number may vary over a wide range.

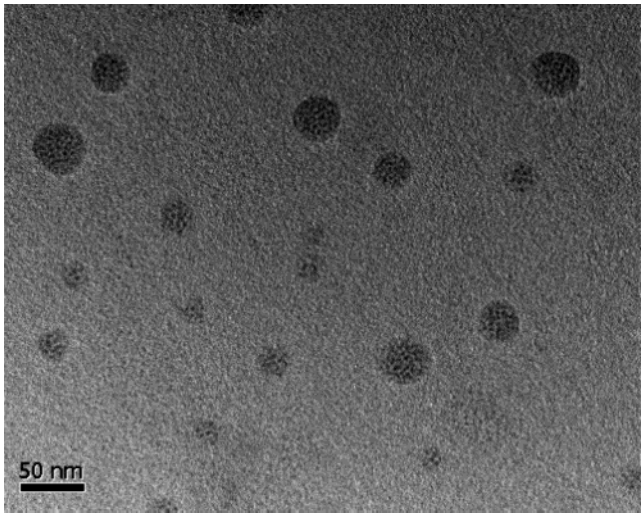

Figure 9. TEM image of P(MAA-*b*-EA) micelles (sample prepared from 0.1 wt % aqueous solution of P(MAA-*b*-EA) at $\alpha = 0.15$).

Transmission Electron Microscope (TEM) Studies. Transmission electron microscopic studies were also carried out to investigate the microstructure of the P(MAA-*b*-EA) micelle. The sample was prepared on a copper grid precoated with carbon and stained with osmium tetraoxide (OsO_4) to enhance the contrast between the micelle and the background. A JEOL JEM-2010 transmission electron microscope operating at 120 kV was used to examine the morphology of the aggregates, and to confirm the proposed micellar structure determined from light scattering studies. The TEM image of the sample prepared from 0.1 wt % aqueous solution of P(MAA-*b*-EA) at $\alpha = 0.15$ is shown in Figure 9. Spherical particles with smooth surface and uniform size were observed, and they represent the micellar aggregates. The radii of the micelles vary from ~12 to ~23 nm, which is slightly smaller than the particle size obtained from dynamic light scattering ($R_h \sim 30$ nm). The smaller particle size is caused by the shrinkage of micelles when the solvent evaporates during sample preparation. It is noted that the shrinkage is not significant, indicating that the polymer chains may not be considerably solvated at low α ($\alpha \leq 0.15$) and the density of micelles is close to unity. This agrees with the light scattering results showing that R_h and R_g have nearly identical values and the second virial coefficient is negative in the early stage of neutralization ($\alpha = 0-0.15$). A micrograph focusing on one individual micelle is shown in Figure 10, in which a micelle with core−shell structure can be roughly visualized. The color of the center of the micelle is apparently darker than that of the outer layer, characterizing a micellar core of higher density that is constituted by the EA blocks and unneutralized MAA segments, and a shell layer composed by the neutralized segments of MAA blocks. The proposed micellar structure of the P(MAA-*b*-EA) polymer at different α values based on the light scattering and TEM studies is illustrated in Figure 11.

Conclusions

The association behavior of P(MAA-*b*-EA) block copolymer was examined using potentiometric titration, LLS, and TEM and compared with random and cross-linked MAA−EA copolymers. The P(MAA-*b*-EA) block copolymers exist as spheri-

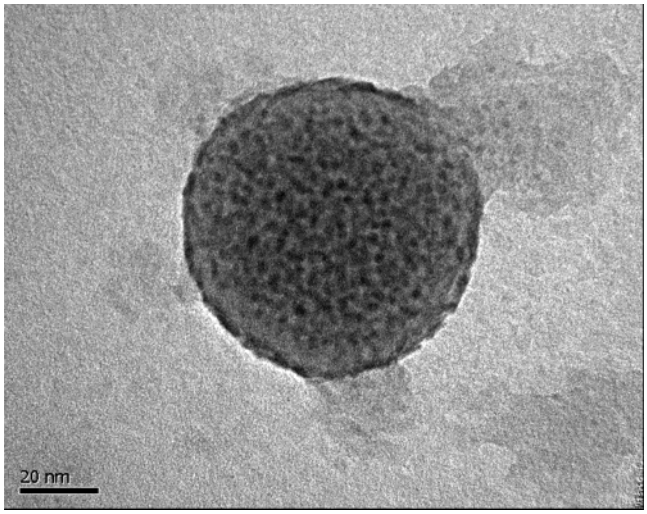

Figure 10. TEM micrograph of P(MAA-*b*-EA) micelle under higher magnification.

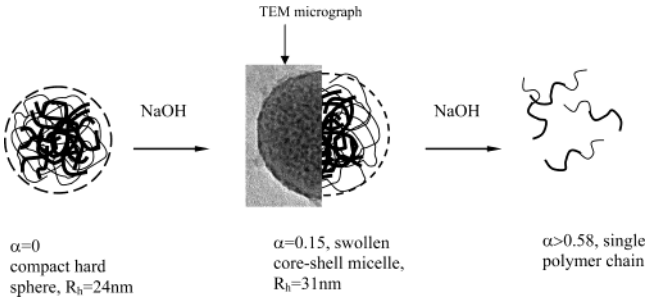

Figure 11. Proposed micellar structure of the P(MAA-*b*-EA) polymer at different α values.

cal micelles consisting of a hydrophobic EA core surrounded by a hydrophilic MAA shell with a particle size (R_h) of 20−30 nm and aggregation number ∼60−75. The pK_a of P(MAA-*b*-EA) copolymer exhibits a slope change and the particle size exhibits a maximum in the range of α from 0.07 to 0.28, suggesting a conformational change (expansion−dissociation) of the polymer upon ionization. The micelles completely disintegrate into single polymer chains at $\alpha = 0.6$, driven by the overwhelming electrostatic repulsion within carboxylate groups. It is also found that the low glass transition temperature (T_g) of the EA block (−31 °C) results in a fast polymer chain exchange between micelles and unimers. On the other hand, the P(MAA-*b*-MMA) retains its micellar structure even when the chains are highly charged at $\alpha = 1$, which is caused by high T_g of MMA blocks causing low chain mobility and results in the formation of frozen micelles.

Acknowledgment. R.P. acknowledges the financial support for the postdoctoral fellowship provided by the Singapore-MIT (SMA) Alliance.

References and Notes

(1) Urban, D.; Gerst, M.; Rossmanith, P.; Schuch, H. *Polym. Mater. Sci. Eng.* **1998**, *79*, 440.
(2) Sukhorukov, G. B.; Antipov, A. A.; Vogit, A.; Donath, E.; Mohwald, H. *Macromol. Rapid Commun.* **2001**, *22* (1), 44.
(3) Sauer, M.; Meier, W. *Chem. Commun.* **2001**, *1*, 55.
(4) Zhang, X.; Matyjaszewski, K. *Macromolecules* **1999**, *32*, 1763.
(5) Winnik, M. A.; Yekta, A. *Curr. Opin. Colloid Interface Sci.* **1997**, *2* (4), 424.
(6) Hamley, I. W. *The Physics of Block Copolymers*; Oxford University Press: Oxford, U.K., 1998.
(7) Klok, H. A.; Lecommandoux, S. *Adv. Mater.* **2001**, *13*, 1217.
(8) Benahmed, A.; Ranger, M.; Leroux, J. *Pharm. Res.* **2001**, *18* (3), 323.
(9) Eisenberg, A.; Rinaudo, M. *Polym. Bull.* **1990**, *24* (6), 671.
(10) Moffit, M.; Khougaz, K.; Eisenberg, A. *Acc. Chem. Res.* **1996**, *29* (2), 95.
(11) Schuch, H.; Klingler, J.; Rossmanith, P.; Frechen, T.; Gerst, M.; Feldthusen, J.; Müller, A. H. E. *Macromolecules* **2000**, *33*, 1734.
(12) Stepanek, M.; Podhajecka, K.; Tesarova, E.; Prochazka, K.; Tuzar, Z.; Brown, W. *Langmuir* **2001**, *17* (14), 4240.
(13) Zhang, L. F.; Eisenberg, A. *Science* **1995**, *268* (5218), 1728.
(14) Zhang, L. F.; Barlow, R. J.; Eisenberg, A. *Macromolecules* **1995**, *28*, 6055.
(15) Zhang, L. F.; Eisenberg, A. *J. Am. Chem. Soc.* **1996**, *118*, 3168.
(16) Ranger, M.; Jones, M.; Yessine, M.; Leroux, J. *J. Polym. Sci.: Part A: Polym. Chem.* **2001**, *39*, 3861.
(17) Cheng, G.; Böker, A.; Zhang, M.; Krausch, G.; Müller, A. H. E. *Macromolecules* **2001**, *34*, 6883.
(18) Bieringer, R.; Abetz, V.; Müller, A. H. E. *Eur. Phys. J.* **2000**, *5*, 5.
(19) Gohy, J. F.; Willet, N.; Varshney, S.; Zhang, J. X.; Jerome, R. *Angew. Chem., Int. Ed.* **2001**, *40* (17), 3214.
(20) Talingting, M. R.; Munk, P.; Webber, S. E.; Tuzar, Z. *Macromolecules* **1999**, *32* (5), 1593.
(21) Cao, T.; Munk, P.; Ramireddy, C.; Tuzar, Z.; Webber, S. E. *Macromolecules* **1991**, *24*, 6300.
(22) Prochazka, K.; Kiserow, D.; Ramireddy, C.; Tuzar, Z.; Munk, P.; Webber, S. E. *Macromolecules* **1992**, *25*, 454.
(23) Tuzar, Z.; Kratochvil, P.; Prochazka, K.; Munk, P. *Collect. Czech. Chem. Commun.* **1993**, *58*, 2362.
(24) Wise, D. L.; Trantole, D. J.; Altobelli, D. E.; Yaszemski, M. J.; Gresser, J. D.; Schwartz, E. R. *Encyclopedic Handbook of Biomaterials and Bioengineering, Part A: Materials*; Marcel Dekker: New York, 1995; Vol. 2.
(25) Wang, C.; Tam, K. C.; Jenkins, R. D.; Bassett, D. R. *Phys. Chem. Chem. Phys.* **2000**, *2*, 1967.
(26) Wang, C.; Tam, K. C.; Jenkins, R. D. *J. Phys. Chem. B* **2002**, *106* (6), 1195.
(27) Gan, L. H.; Ravi, R.; Mao, B. V.; Tam, K. C. *J. Polym. Sci.: Part A: Polym. Chem.* **2003**, *41* (17), 2688.
(28) Zhang, X.; Xia, J.; Matyjaszewski, K. *Polym. Prepr.* (*Am. Chem. Soc., Div. Polym. Chem.*) **1999**, *40* (*2*), 440.
(29) Leyte, J. C.; Mandel, M. *J. Polym. Sci.* **1964**, *2*, 1879.
(30) Ochiai, H.; Anabuki, Y.; Kojima, O.; Tominaga, K.; Murakami, I. *J. Polym. Sci., Part B: Polym. Phys.* **1990**, *28*, 233.
(31) Hirose, Y.; Sakamoto, Y.; Tajima, H.; Kawaguchi, S.; Ito, K. *J. Phys. Chem.* **1996**, *100*, 4612.
(32) Mandel, M.; Leyte, J. C. *Electroanal. Chem.* **1972**, *33*, 297.
(33) Barone, G.; Virgilio, N. D.; Elia, V.; Rizzo, E. *J. Polym. Sci.* **1974**, *44*, 1.
(34) Dubin, P.; Strauss, U. P. *J. Phys. Chem.* **1970**, *74*, 2842.
(35) Dubin, P.; Strauss, U. P. *J. Phys. Chem.* **1973**, *77*, 1427.
(36) Hermans, J., Jr. *J. Phys. Chem.* **1966**, *70*, 510.
(37) Ravi, P.; Wang, C.; Tam, K. C.; Gan, L. H. *Macromolecules* **2003**, *36*, 173.
(38) Booth, C.; Atwood, D. *Macromol. Rapid Commun.* **2000**, *21* (9), 501.